Emilio Gomez-Gonzalez, PhD *‡
Francisco Javier Munoz-Gonzalez, ME *
Alejandro Barriga-Rivera, PhD *§
Manuel A. Perales-Esteve, PhD ||
Manuel Guerrero-Claro, ME*
Isabel Fernandez-Lizaranzu, ME *‡
Desirée Requena-Lancharro, BE *
Marina Rosales-Martinez, PhD *
Javier Marquez-Rivas, MD, PhD *‡¶

(Continued on next page)

As detailed in the Funding paragraph, this study was developed within the EU H2020 ATTRACT Project. The overall objectives and results were presented as a report at the ATTRACT Final Conference (Online Conference, Sept 22, 2020): https://phase1.attract-eu.com/showroom/project/combined-optical-imaging-and-ultrasound-focusing-for-hand-held-non-invasive-cleaning-of-implanted-cerebrospinal-fluid-shunting-devices-in-patients-of-hydrocephalus-initial-design-and-proof-of-concep/. The contents in this manuscript are not included in the aforementioned presentation.

Correspondence:
Emilio Gomez-Gonzalez, PhD,
Department of Applied Physics III,
School of Engineering,
University of Seville,
Camino de los Descubrimientos s/n,
41092 Sevilla, Spain.
Email: egomez@us.es

Received, January 11, 2022.
Accepted, May 24, 2022.
Published Online, September 19, 2022.

OPEN

Contactless Ultrasonic Cavitation for the Prevention of Shunt Obstruction in Hydrocephalus: A Proof-of-Concept Study

BACKGROUND: Obstructive failure of implanted shunts is the most common complication in the treatment of hydrocephalus. Biological material and debris accumulate in the inner walls of the valve and catheters block the normal flow of the drained cerebrospinal fluid causing severe symptoms with high morbidity and mortality. Unfortunately, at present, there is no effective preventive protocol or cleaning procedure available.
OBJECTIVE: To assess whether externally applied, focused ultrasound beams can be used to resuspend deposits accumulated in brain shunts safely.
METHODS: A computational model of an implanted brain shunt was implemented to test the initial design parameters of a system comprising several ultrasound transducers. Under laboratory conditions, configurations with 3 and 4 transducers were arranged in a triangle and square pattern with their radiation axis directed towards a target model of the device, 2 catheters and a brain shunt filled with water and deposited graphite powder. The ultrasound beams were then concentrated on the device across a head model.
RESULTS: The computational model revealed that by using only 3 transducers, the acoustic field intensity on the valve was approximately twice that on the brain surface suggesting that acoustic cavitation could be selectively achieved. Resuspension of graphite deposits inside the catheters and the valve were then physically demonstrated and video-recorded with no temperature increase.
CONCLUSION: The technology presented here has the potential to be used routinely as a noninvasive, preventive cleaning procedure to reduce the likelihood of obstruction-related events in patients with hydrocephalus treated with an implanted shunt.

KEY WORDS: Hydrocephalus, Shunt cleaning, Ultrasound cavitation, Valve obstruction, Ventricular catheter, Cerebrospinal fluid

Operative Neurosurgery 23:420–426, 2022 https://doi.org/10.1227/ons.0000000000000372

The abnormal accumulation of fluids in the brain, known as hydrocephalous, is a severe health condition[1] that affects patients of all age groups.[2-4] It comprises a wide set of ailments associated with alterations in the cerebrospinal fluid (CSF) hydrodynamics and the biomechanical properties of the structures of the central nervous system. In many cases, these pathologies are characterized by an enlargement of the lateral ventricles of the brain, caused by the accumulation of CSF, and by the physiological and cognitive consequences of the compression of the brain structures produced by the increased intracranial pressure.[5] Symptoms range from fatigue or memory problems to loss of cortical functions (speech, motion, vision, etc), and if untreated, it can lead to death.[6,7] Normally, clinical management of hydrocephalus requires the neurosurgical implantation of a brain shunt to drain the CSF excess.[8,9] Unfortunately, shunt failures are common[10-12] and can lead to life-threatening medical situations if not rapidly replaced.[13,14] In a recent review, Paff et al[15] stated that the most frequent cause of shunt malfunction was the obstruction of the implant. Although this obstruction can occur at any point along the brain shunt, the authors concluded that the implant is most likely to be clogged at the proximal catheter. At present, there is no clear consensus on the cause of the brain shunt blockade; it may be explained by particles of brain parenchyma[16] or fragments of the choroid

Supplemental digital content is available for this article at operativeneurosurgery-online.com.

plexus[17] clogging the luminal space or by a progressive buildup of other tissue debris, proteins, or blood cells producing an eventual occlusion.[18,19] Although there are no preventive technologies or medical approaches to avoid such complications in the long term,[20] refinement of the surgical technique can decrease rates of infection in the short term.[21,22]

There have been different attempts to devise a method to clear blocked shunts: thermal cauterization of the obstruction,[23] delivery of high-energy laser pulses using fiber optics,[24,25] and generation of cavitation by delivering ultrasonic waves from a transducer coupled to a wire.[26] All these techniques require positioning a probe inside the shunt in the proximity of the blockade to locally deliver energy thus compromising the patency of the catheter and increasing substantially the temperature of the treated area. Although these techniques possess clear benefits over surgical replacement, the inherent risks associated with the insertion of a probe within the luminal space of the shunt restrict the use of these technologies to shunt failure events. By contrast, this study presents a proof of concept of a contactless technology to prevent shunt blockade. In a laboratory model of a patient head, by delivering focused ultrasound[27] from an external array of piezoelectric transducers, we generated cavitation within the device causing the resuspension of the deposited materials with minimal temperature increase.

METHODS

A laboratory prototype was implemented to test whether contactless cavitation and reflow of adhered material could be achieved in brain shunts. In doing so, the first step was to build a 3-dimensional (3D) computational model to optimize ultrasound focusing within the targeted volume of interest while reducing energy transfer onto surrounding area. Then, an array of ultrasonic transducers, distributed to concentrate the ultrasound beams within a model of an occluded brain shunt, were used to demonstrate the viability of the technology proposed in this study.

Computational Model

A 3D computational model was built using COMSOL Multiphysics v.5.3a (COMSOL Inc) with different material properties[28-33] (see details in the **Supplemental Digital Content**, http://links.lww.com/ONS/A786). In brief, the emitters were modeled as dipolar sources firstly and, thereafter, as vibrating surfaces, and the acoustic fields were obtained by solving the Helmholtz equation in the frequency domain using the acoustic module provided. Further details on the model equations and parameters are given in the **Supplemental Digital Content**, http://links.lww.com/ONS/A786. The model was solved within a simplified geometrical representation of an implanted brain shunt over a flat cranial surface of a 200 × 200 mm^2, as shown in Figure 1. The biological domains included a layer of white matter (50 mm), gray matter (20 mm), cranial bone (6 mm), a thin layer of scar tissue surrounding the implant (1 mm), skin (2.5 mm), and CSF within the shunt. The geometry of the implant was obtained by generating a surface of revolution from the contour of a Codman–Hakim programmable valve (Codman, Johnson & Johnson Co.). Three ultrasonic transducers were modeled as 1-cm thick hollow cylinders with the radiation axis directed toward the center of the valve using different angular configurations. The acoustic pressure (expressed in Pa) and the acoustic intensity (expressed in $W \cdot m^{-2}$) fields were then computed at 39 kHz, 40 kHz, and 41 kHz.

Shunt Obstruction Model

A simplified model of a brain catheter was built from transparent polyvinyl chloride conduits with inner diameters of 1 mm, 3 mm, and 10 mm. The tube was filled with a mix of water and graphite powder to generate high-quality videos (Videos 1 and 2) demonstrating contactless ultrasonic cavitation. A second fluid was prepared to simulate drained CSF from patients with conditions, ie, severe infections or hemorrhages among others, affecting the shunt flow. For that purpose, water was mixed with 30% egg white to form a colloidal solution with high protein content. These proteinaceous preparations were left to dry within the tubes for no less than 15 days to mimic the blocking deposits causing shunt failures.

In addition, ultrasonic cavitation was also demonstrated in a Codman-Hakim valve. It has to be noted that catheters used in conventional procedures are made of opaque medical-grade silicone. Therefore, demonstration of successful cavitation was limited to the interior of the valve and to nonmedical grade translucid plastic tubing. The experiments were conducted under standard laboratory conditions for temperature and humidity, approximately 22 °C and 50%, respectively.

Ultrasound Focusing

Four HS-4SH-3840 ultrasonic transducers (Hesentec) were arranged with their principal radiation axis directed toward the targeted area of the shunt model. The transducer array was powered by an ultrasonic frequency generator SET 1700W (TimeTech GmbH). The transducers were arranged in a square with 60 mm side and its center located approximately at 140 mm above the target volume to maximize focusing. All transducers were positioned with their radiation axis directed toward the sample. To demonstrate cavitation, ultrasonic radiation was applied during 30 seconds with total electric power of 60 W equally split over the 4 transducers in the array. Note that the shunt model was placed under water, and the radiating surfaces of the transducers were also immersed to mimic the use of a coupling gel. The process was recorded at 60 frames per second using a Blackmagic Micro Cinema Camera (Blackmagic Design) mounting a Rokinon 35 mm T1.5 Cine AS UMC lens (Samyang Optics). In addition, temperature was monitored using a thermocouple TESTO 925 (Testo) with a 4-mm diameter probe inserted in the target area.

Ethics Assessment

The described research does not include the use of human participants or animal subjects. It does not require approval by Institutional Review Board nor Ethics Committee. No patient consent form is needed.

(Continued from previous page)

*Department of Applied Physics III, ETSI School of Engineering, University of Seville, Sevilla, Spain; ‡Group of Applied Neuroscience, Institute of Biomedicine of Seville, Sevilla, Spain; §School of Biomedical Engineering, The University of Sydney, Sydney, NSW, Australia; ||Department of Electronic Engineering, ETSI School of Engineering, University of Seville, Sevilla, Spain; ¶Service of Neurosurgery, University Hospital 'Virgen del Rocio', Sevilla, Spain

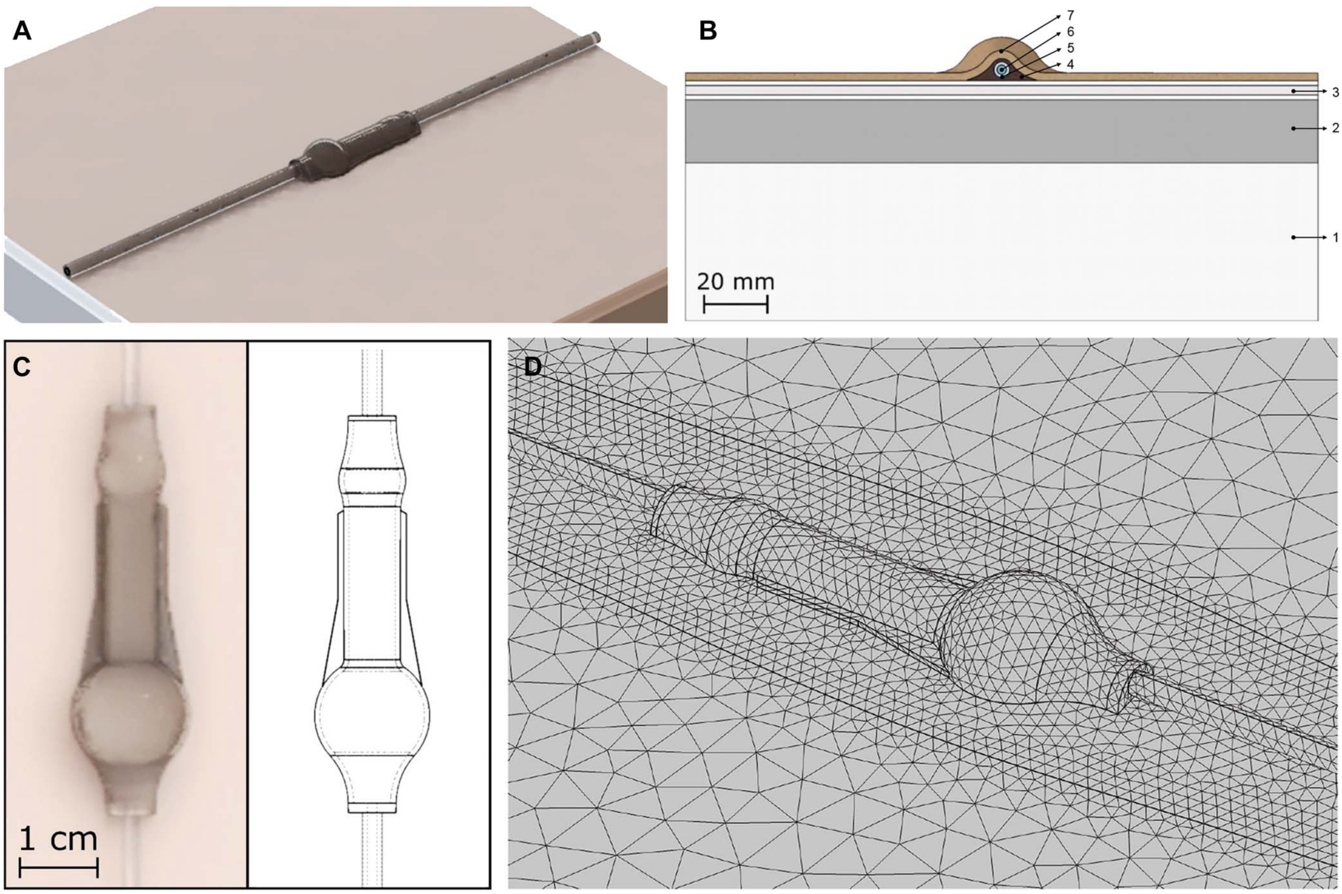

FIGURE 1. *Illustration of the geometry used in the computation model.* **A**, *A 3D rendering of the geometric structures.* **B**, *A cross-sectional area of the 3D domains containing the different layers considered in the model formulation. 1: White matter, 2: gray matter, 3: cranial bone, 4: scar tissue, 5: implanted brain shunt, 6: cerebrospinal fluid, and 7: skin.* **C**, *The shunt used to render the 3D model.* **D**, *The mesh used in the 3D valve model. 3D, 3-dimensional*

RESULTS

A prototype of a device able to generate contactless ultrasonic cavitation in a standard hydrocephalus shunt has been designed, and its application for noninvasive cleaning by removal of adhered deposits has been computationally and experimentally demonstrated and video-recorded in a physical laboratory setup. For that purpose, different transducer configurations were analyzed using the computational model previously described. Figure 2A shows final configuration with which the results had been obtained. This tool allows for adjusting the position of the transducers and the frequency of the radiation to maximize focusing of the acoustic energy on the obstructed shunt while reducing the amount of energy transferred onto surrounding tissues and structures. Figure 2B shows the results of the initial study conducted to assess whether higher intensities of acoustic energy could be locally delivered over the blocked shunt in a conceptually similar way as it is used for the treatment of tumors.[34] Although ablation of tumors is achieved because of the temperature increase produced by high-intensity ultrasounds, intended cavitation can be induced using low-intensity ultrasonic waves at lower frequencies, as commonly used in cleaning devices[35] for industrial applications. Along these lines, the model revealed that a high degree of ultrasound focusing could be achieved at approximately 40 kHz with the elements of the array arranged symmetrically around the target. Note that a high-intensity node was demonstrated at 41 kHz with a 30° angle configuration in the proximity of the shunt.

After initial tests, the model was then reformulated to induce a relatively high level of acoustic intensity accurately focused on the valve. For that purpose, the transducers were arranged in a 45° angle configuration with ultrasound frequency set to 40 kHz, as shown in Figure 3. The acoustic intensity thus obtained over the shunt was between 2 and 3 times larger than that obtained on the surface of the brain, as illustrated in Figure 3A. The intensity pattern thus achieved was highly localized on the model of the shunt, as shown in Figure 3B. An additional configuration is presented in the

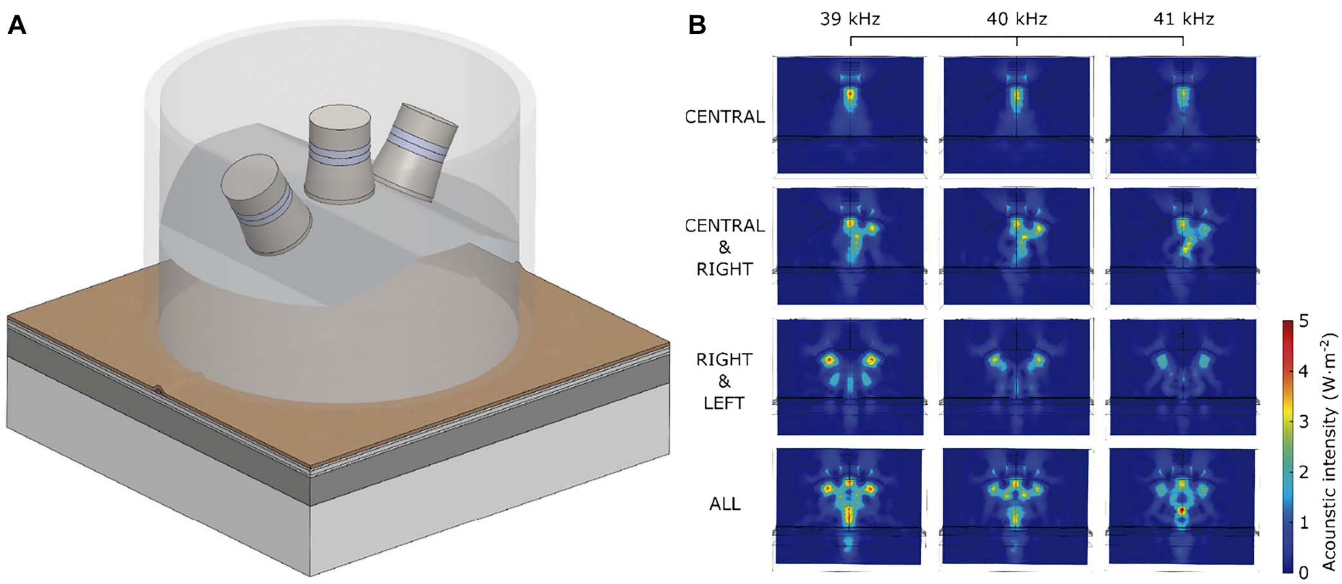

FIGURE 2. A, *A 3-dimensional rendering of the geometrical configuration used here.* B, *The acoustic intensity fields obtained from different transducer configurations. Three different ultrasound frequencies were used. The transducers were position with their radiation axis in a 30° angle configuration relative to the vertical line. A high-intensity node was induced when all transducers were activated at 41 kHz. The amplitude of the emitters was set to 1 MN* m^{-3}.

Supplemental Digital Content, http://links.lww.com/ONS/A786, with the lateral transducers in a 35° and 55° configurations. Ultrasonic energy appeared focused on the proximal site.

Stemming from these preliminary results on the geometrical distribution of the acoustic intensity, we sought to experimentally demonstrate, on the bench, whether low-intensity ultrasonic cavitation could be induced inside a real shunt. Graphite deposits within the catheter and the valve were resuspended using 4 ultrasound transducers symmetrically distributed above the center of the sonication volume. Figures 4 and 5 show details of said cavitation within a catheter and a valve, respectively, using images extracted from recorded videos files (Videos 1 and 2). At t = 0, the graphite tracer was deposited on the lower walls of the devices. After activation of the ultrasound, the particles commenced to emerge and then diffused within the fluid only in the target volume (Figures 4 and 5, and Videos 1 and 2). During the sonication time, no temperature increase was detected above the resolution of the sensor. Similarly, albumin deposits were successfully re-flown when using high-protein fluid media. Experimental demonstrations are recorded in 2 full-length videos (Videos 1 and 2).

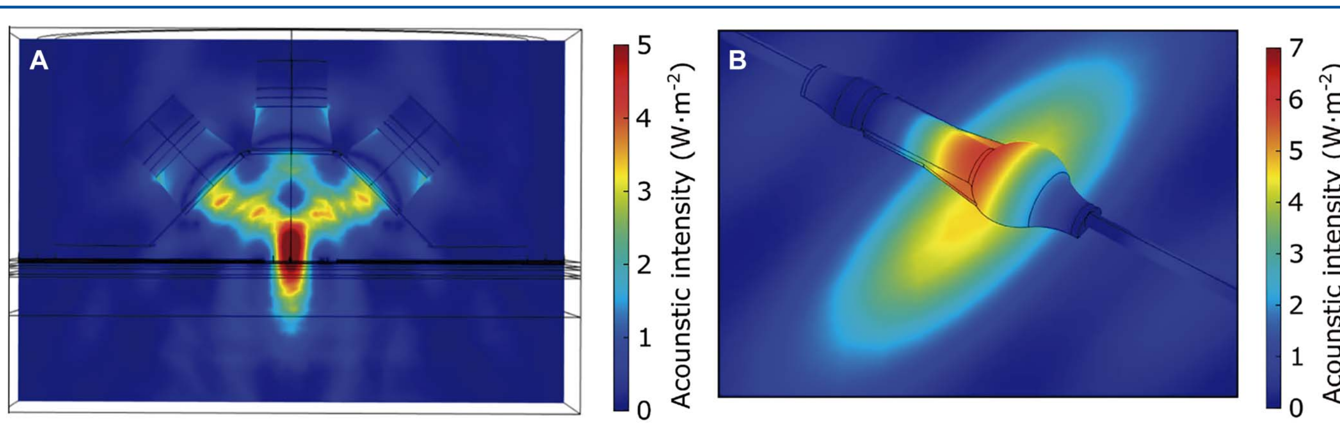

FIGURE 3. A, *The acoustic intensity field obtained at 40 kHz in a 45° configuration with the 3 transducers activated simultaneously.* B, *A detail of the acoustic intensity field within the model of the shunt. The amplitude of the emitters was set to 1 MN* m^{-3}.

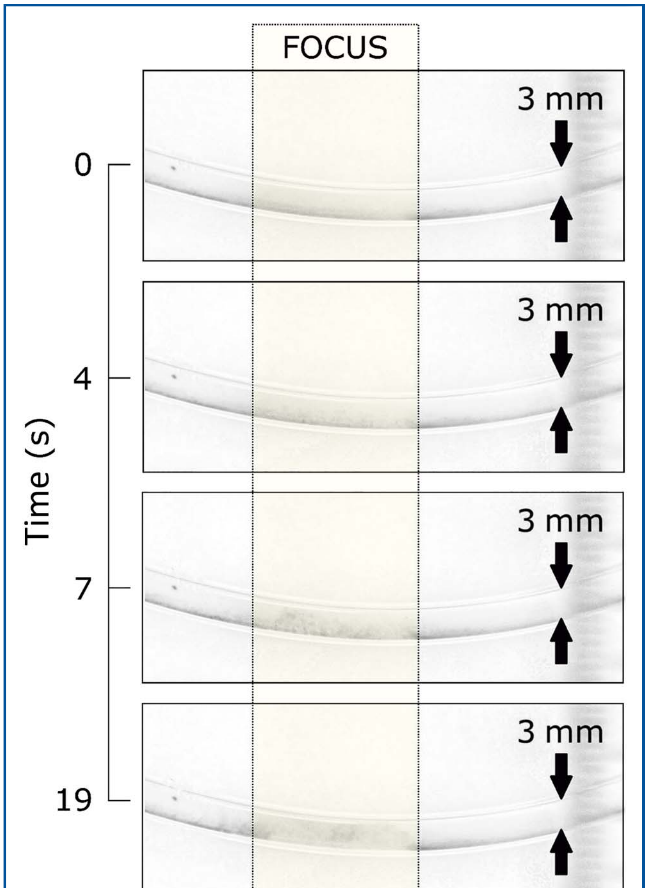

FIGURE 4. *Selection of photograms from demo video (Video 1) demonstrating cavitation within a 3-mm catheter filled with water and graphite powder. The graphite tracer can be observed at t = 0 deposited on the lower wall of the catheter in the absence of ultrasonic waves. The remaining photograms illustrate resuspension of the graphite particles.*

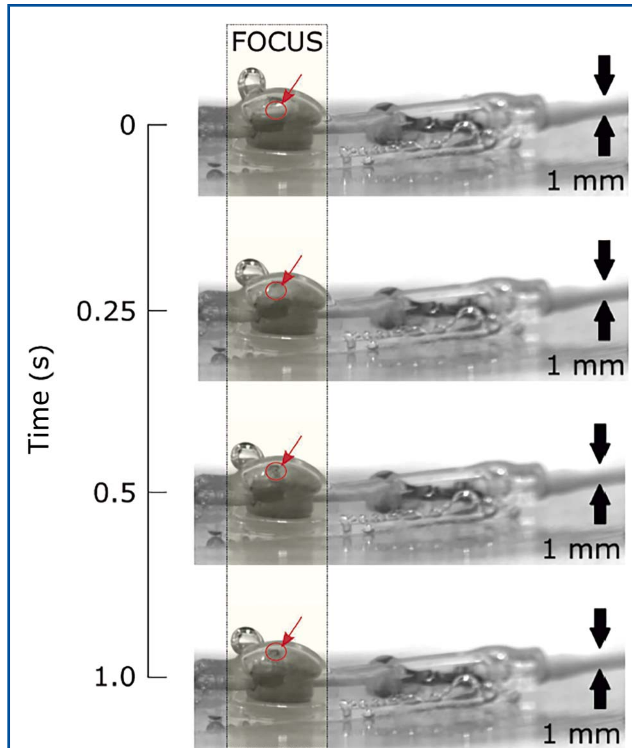

FIGURE 5. *Selection of photograms from demo video (Video 2) demonstrating cavitation inside a hydrocephalus valve filled with water and graphite powder over. The graphite tracer at t = 0 is deposited on the lower wall of the valve in the absence of ultrasonic waves. The remaining photograms illustrate resuspension of the graphite particles within 1 second of ultrasonic radiation.*

DISCUSSION

The most frequent treatment for hydrocephalus relies on implanting a shunt—composed of 2 catheter segments and a valve—to drain cerebrospinal fluid from brain ventricles to a distal cavity.[8,9] As device failure remains one of the major limitations of the therapy,[10-12] the scientific community has sought ways of restoring flow by delivering optical,[24,25] acoustic,[26] or thermal energy[23] to achieve removal of blocking deposits. To date, state-of-the-art technologies require inserting a probe within the device to break down the blockade. First attempts to use ultrasonic cavitation date from 2001.[36] At that time, Ginsberg et al[26] described a device able to recanalize obstructed devices delivering 20-kHz ultrasonic waves from a probe inserted percutaneously in the shunt. One of the problems the initial design they reported was a temperature increase around the transducer able to trigger protein denaturalization.[26] Although it was mitigated by saline irrigation, there were other important risks associated with this device, such as the potential to harm the brain if the occlusion was located proximal to the valve.

The method presented here provides a noninvasive approach that might prevent failures. As this technology can produce contact-less cavitation within the target volume, it has the potential to be used routinely to remove the accumulation of biological deposits before they block the normal flow, particularly in the valve. However, as blockades tend to occur most frequently at the proximal catheter, the ultimate challenge lies with clearing plugged biological material in close proximity to sensitive brain tissue. Note that the use of multiple ultrasound transducers allows for creating regions of relatively high acoustic intensity able to induce cavitation locally while reducing overheating of the surrounding tissues, as demonstrated herein.

Limitations

High-intensity focused ultrasound has been extensively used in neurosurgery for noninvasive treatment of brain tumors[37] among others. The idea underlying this study was inspired on said applications,[38] but using lower acoustic energy and frequency instead. The ultimate goal was, therefore, to produce cavitation only with a minimum temperature increase. For these reasons, we chose frequencies in the range of 30 to 100 kHz, as they have a demonstrated capacity for generating cavitation bubbles without tissue heating.[39] Nevertheless, the frequency, the number of transducers, and their relative positions need to be further studied in preclinical studies before developing a prototype for clinical trials. Note this study has demonstrated the feasibility of the technique in a laboratory setup using a relatively simple configuration and, therefore, statements on safety cannot be made at this instance. Without hesitation, the next steps should aim at verifying whether ultrasonic energy, focused in the fashion described here, disrupts the neighboring brain tissue. It can be anticipated that special attention will be required when delivering ultrasonic energy to the proximal catheter. A strategy for minimizing potential tissue harm would require the use of multiple ultrasonic sources. Note that although the real anatomy is substantially more complex, it is expected that the degree of ultrasound focusing improves with larger numbers of transducers. Optimization of the energy delivery process can be assisted by the use of artificial intelligence.[40] This together would reduce the energy required from each transducer and the amount of energy delivered during treatment while achieving more localized cavitation in the desired volume.

CONCLUSION

In this work, we present a computational and experimental proof-of-concept of the use of externally applied focused ultrasound to remove accumulated debris in models of implanted brain shunts and to improve cerebrospinal fluid flow through valves and catheters. This procedure may be used for noninvasive, preventive, cleaning of implanted shunts in patients with hydrocephalus.

Funding

This paper is part of ATTRACT that has received funding from the European Union's Horizon 2020 Research and Innovation Programme (under Grant Agreement Number 777222). The Consortium Partners of ATTRACT are not responsible for any use that may be made of the results. In addition, this article reflects only the authors' views and not necessarily those of said Consortium Partners. This research has also been partially funded by the Project "Innovative Ecosystem with Artificial Intelligence for Andalusia 2025" of the Autonomous Government of Andalusia, Spain, in the International Campus of Excellence "Andalucia-Tech" of the University of Malaga and the University of Seville (reference CEI-11) and for the 'Fundacion para la Innovacion y la Prospectiva de Salud en España' (FIPSE, ref. 3734-20). ABR was supported by Grant Number RTI2018-094465-J-I00 funded by MICIN/AEI/10.13039/501100011033 and by "ERDF A way of making Europe."

Disclosures

E. Gomez-Gonzalez, J. Marquez-Rivas, M. A. Perales-Esteve, M. Guerrero-Claro, F. J. Munoz-Gonzalez, and I. Fernandez-Lizaranzu have filed a patent application related to this technology. The other authors have no personal, financial, or institutional interest in any of the drugs, materials, or devices described in this article.

REFERENCES

1. Rekate HL. A contemporary definition and classification of hydrocephalus. *Semin Pediatr Neurol.* 2009;16(1):9-15.
2. Kahle T, Kulkarni V, Limbrick D, Warf C. Hydrocephalus in children. *Lancet.* 2002;387(10020):788-799.
3. Vinchon M, Baroncini M, Delestret I. Adult outcome of pediatric hydrocephalus. *Child's Nervous Syst.* 2012;28(6):847-854.
4. Isaacs A, Riva-Cambrin J, Yavin D, et al. Age-specific global epidemiology of hydrocephalus: systematic review, metanalysis and global birth surveillance. *PLoS One.* 2018;13(10):e0204926.
5. Hakim S, Venegas JK, Burton JD. The physics of the cranial cavity, hydrocephalus and normal pressure hydrocephalus: mechanical interpretation and mathematical model. *Surg Neurol.* 1976;5(3):187-210.
6. Gholampour S, Fatouraee N, Seddighi AS, Seddighi A. Evaluating the effect of hydrocephalus cause on the manner of changes in the effective parameters and clinical symptoms of the disease. *J Clin Neurosci.* 2017;35:50-55.
7. Kirkpatrick M, Engleman H, Minns R. Symptoms and signs of progressive hydrocephalus. *Arch Dis Child.* 1989;64(1):124-128.
8. Drake JM, Kestle JR, Milner R, et al. Randomized trial of cerebrospinal fluid shunt valve design in pediatric hydrocephalus. *Neurosurgery.* 1998;43(2):294-303.
9. Salmon JH. Adult hydrocephalus: evaluation of shunt therapy in 80 patients. *J Neurosurg.* 1972;37(4):423-428.
10. Khan F, Rehman A, Shamim MS, Bari ME. Factors affecting ventriculoperitoneal shunt survival in adult patients. *Surg Neurol Int.* 2015;6:25.
11. Borgbjerg B, Gjerris F, Albeck M, Hauerberg J, Børgesen S. Frequency and causes of shunt revisions in different cerebrospinal fluid shunt types. *Acta Neurochir.* 1995; 136(3-4):189-194.
12. Drake J, Kestle J, Tuli S. CSF shunts 50 years on–past, present and future. *Child's Nerv Syst.* 2000;16(10-11):800-804.
13. Bryant M, McEniery J, Walker DG, et al. Preliminary study of shunt related death in paediatric patients. *J Clin Neurosci.* 2004;11(6):614-615.
14. Do N, Hill KD, Wallace AS, Vricella L, et al. Shunt failure—risk factors and outcomes: an analysis of the Society of Thoracic Surgeons Congenital Heart Surgery Database. *Ann Thorac Surg.* 2018;105(3):857-864.
15. Paff M, Alexandru-Abrams D, Muhonen M, et al. Ventriculoperitoneal shunt complications: a review. *Interdiscip Neurosurg.* 2018;13:66-70.
16. Kehler U, Klöhn A, Heese O, et al. Hydrocephalus therapy: reduction of shunt occlusions using a peel-away sheath. *Clin Neurol Neurosurg.* 2003;105(4):253-255.
17. Dickerman RD, McConathy WJ, Morgan J, et al. Ailure rate of frontal versus parietal approaches for proximal catheter placement in ventriculoperitoneal shunts: revisited. *J Clin Neurosci.* 2005;12(7):781-783.
18. Brydon HL, Bayston R, Hayward R, Harkness W. The effect of protein and blood cells on the flow-pressure characteristics of shunts. *Neurosurgery.* 1996;38(3): 498-505.
19. Occhipinti E, Carapella CM. Shunt failure in hydrocephalus with high-protein fluid. *Shunts Probl Shunts.* 1982;8:220-222.
20. Stein SC, Guo W. Have we made progress in preventing shunt failure? A critical analysis. *J Neurosurg Pediatr.* 2008;1(1):40-47.
21. Isaacs AM, Ball CG, Sader N, et al. Reducing the risks of proximal and distal shunt failure in adult hydrocephalus: a shunt outcomes quality improvement study. *J Neurosurg.* 2021;136(3):877-886.
22. Lim J, Tang A, Liles C, et al. The cost of hydrocephalus: a cost-effectiveness model for evaluating surgical techniques. *J Neurosurg Pediatr.* 2018;23(1):109-118.
23. Pattisapu JV, Trumble ER, Taylor KR, Howard PD, Kovach TM. Percutaneous endoscopic recanalization of the catheter: a new technique of proximal shunt revision. *Neurosurgery.* 1999;45(6):1361-1367.
24. Christens-Barry WA, Guarnieri M, Carson BS. Fiberoptic delivery of laser energy to remove occlusions from ventricular shunts: technical report. *Neurosurgery.* 1999; 44(2):345-349.
25. Hutchens TC, Gonzalez DA, Hardy LA, McLanahan CS, Fried NM. Thulium fiber laser recanalization of occluded ventricular catheters in an ex vivo tissue model. *J Biomed Opt.* 2017;22(4):48001.
26. Ginsberg HJ, Drake JM, Peterson TM, Cobbold RS. Recanalization of obstructed cerebrospinal fluid ventricular catheters using ultrasonic cavitation. *Oper Neurosurg.* 2006;59(4 suppl 2):ONS403-ONS412.
27. Hill C, Ter Haar G. High intensity focused ultrasound—potential for cancer treatment. *Br J Radiol.* 1995;68(816):1296-1303.
28. COMSOL Multiphysics® v.5.3a. COMSOL AB. Accessed: January 11, 2022. www.comsol.com.
29. Mueller JK, Legon W, Tyler WJ. Analysis of transcranial focused ultrasound beam profile sensitivity for neuromodulation of the human brain. *arXiv.* 2015;1-32.

30. Feldmann A, Wili P, Maquer G, Zysset P. The thermal conductivity of cortical and cancellous bone. *Eur Cells Mater.* 2018;35:25-33.
31. Otani T, Yuichi S. Acoustic properties of cancellous bone and evaluation of bone density. In: *Sociedad española de acústica*. Sociedad Española de Acústica. 2002:1-6.
32. Baumgartner RW. Handbook on neurovascular ultrasound. Karger Medical and Scientific Publishers; 2006.
33. Hill CR, Ramber JC, Ter Haar GR. Physical principles of medical ultrasonics. In: *The Journal of the Acoustical Society of America*. 2nd ed. Vol 116; 2004:2707-2708.
34. Kennedy JE. High-intensity focused ultrasound in the treatment of solid tumours. *Nat Rev Cancer.* 2005;5(4):321-327.
35. Yamashita T, Ando K. Low-intensity ultrasound induced cavitation and streaming in oxygen-supersaturated water: role of cavitation bubbles as physical cleaning agents. *Ultrason Sonochem.* 2019;52:268-279.
36. Ginsberg HJ, Drake J, Cobbold RS. Unblocking cerebrospinal fluid shunts using low frequency ultrasonic cavitation. In: *2001 IEEE Ultrasonics Symposium. Proceedings. An International Symposium*. Vol 2; 2001:1381-1384.
37. Quadri SA, Waqas M, Khan I, et al. High-intensity focused ultrasound: past, present, and future in neurosurgery. *Neurosurg Focus.* 2018;44(2):E16.
38. Valero P, Gomez-Gonzalez E, Sabino A, Valero M, Suarez-Ramos J. Magnetic-resonance-guided focused ultrasound Surgery in the treatment of oncology patients: fundamentals and review of early clinical applications. *Eur Oncol.* 2010;6(2):79-79.
39. Duck F, Leighton T. Frequency bands for ultrasound, suitable for the consideration of its health effects. *J Acoust Soc Am.* 2018;144(4):2490-2500.
40. Gomez-Gonzalez E, Marquez-Rivas J. Artificial intelligence for the optimization of focused ultrasound cleaning of shunts implanted in patients of different pathologies. In: Guadix-Martin J, Lilic M, Rosales-Martinez M eds. *AI knowledge Transfer from the University to Society. Applications in high-impact sectors.* CRC Press; 2022:2-6.

VIDEO 1. A water-filled catheter (3 mm inner diameter, indicated by black arrows) with graphite deposits is placed within a container (also filled with water, to achieve acoustical coupling with the ultrasound emitters). Ultrasound beams are focused in the center region of the catheter, producing controlled cavitation and the removal of deposits. Note that no effect is produced in the surrounding region around the focused target.

VIDEO 2. A standard hydrocephalus valve connected to catheters (1 mm inner diameter, indicated by black arrows) is water-filled and submerged in a container (also filled with water, to achieve acoustical coupling with the ultrasound emitters). The shunt is placed on top of a rigid holder (with a 1 mm glass layer and a 5 mm cork layer) to simulate the skull bone. The region under the holder is also filled with water. An additional plastic tube (7 mm inner diameter) is placed underneath. There are graphite deposits inside the valve and in the larger tube. When the ultrasound beams are focused in the target volume (ie, in the valve), achieved cavitation removes the deposits inside it but no effects are produced in the surrounding region nor in the other tube.

Supplemental digital content *is available for this article at operativeneurosurgery-online.com.*

Supplemental Digital Content. Model Formulation.
Supplemental Table 1. Acoustic parameters of materials.[25-30]
Supplemental Figure 1. Details of the 3D computational model. A, An external view of the model structures including the scar tissue and skin. B and C, The tetrahedral mesh used to solve the acoustic problem in the different regions and layers. Different mesh sizes can be observed. D, A relative position of the valve and transducers.
Supplemental Figure 2. Spatial distribution (planar view) of the pressure field generated by 3 ultraosuind transducers activated simultaneously and arranged in a 30° configuration. The amplitude of the emitters was set to 1 MN m^{-3} to facilitate the visualization of the spatial distribution of the acoustic field.
Supplemental Figure 3. Example of nonsymetric ultrasonic transducer configuration. A, The geometry used in the simulation. B, An example of the acoustic intensity field preferentially focused on the proximal end of the implant.

Arithmometer built by Veuve Payen around 1914 and sold by Darras around 1915; by Ezrdr, Public domain, via Wikimedia Commons